



## Structural, Spectral, Thermodynamic and HOMO, LUMO Analysis of 2, 6 dithenobenzene-3-enyl 3, 5 dimethyl piperidine-4-one: A quantum chemical analysis

SANGEETHA. R. K<sup>1</sup> and AYYAPPAN. S<sup>2\*</sup>

<sup>1</sup>Department of physics, Sri Eshwar College of Engineering, Coimbatore, India.

<sup>2</sup>Department of physics, Government College of Technology, Coimbatore, India.

\*Corresponding author E-mail: ayyappan@gct.ac.in

<http://dx.doi.org/10.13005/ojc/370618>

(Received: September 27, 2021; Accepted: November 05, 2021)

### ABSTRACT

In the current work, the vibrational frequencies, infrared intensities, molecular geometry and Raman scattering were determined and investigated using ab initio Hartree-Fock (HF) and density functional methods with a basis set of 6-311++ G (d, p) of the organic molecule under interpretation. The FT-IR and FT-Raman spectra of titled molecule have been recorded in the region 4000-400 cm<sup>-1</sup> and 5000-70 cm<sup>-1</sup>, respectively. The optimized geometry structures (bond lengths and bond angles) achieved using HF shows the best result with the experimental values of the titled molecule. The frontier molecular orbitals help to distinguish chemical responsiveness and molecular kinetic steadiness, thus HOMO-LUMO analysis can be done using the quantum chemistry to improve thermodynamics. The electron density mapping to electrostatic potential surfaces were involved in finding the reactivity sites of the titled compound. With the help of Gauss view 5.0 and Chemcraft packages, the obtained outputs are analyzed. Hyperpolarizability and non-linear optical effect of isolated molecules of NLO materials are observed to be an extensive tool for molecular spectroscopy research. Therefore, for industrial application, Hyperpolarizability of the molecule is also studied.

**Keywords:** DFT, HF, NBO, HOMO LUMO, NLO.

### INTRODUCTION

The phenomenal developments in ab initio and density functional theory (DFT) over the last decade have made possible efficient and systematic predictions of harmonic vibrational frequencies, together with harmonic dipole strengths and rotational strengths which determine harmonic intensities of fundamental transitions in vibrational non polarized absorption like infra-red (IR) and vibrational circular

dichroism (VCD) spectra. Molecular computational studies can provide a broad understanding of the relationships between molecular architecture, non-linear optical characteristics and bioactivity<sup>1</sup>. Piperidins-4-one and its derivatives are highly determined due to its pharmaceutical applications, including antiviral drugs, anti-tumor drugs<sup>2</sup>, analgesics and local anesthetic<sup>3,4</sup>, bactericides, fungicides, and depressants. It is very sensitive to spectroscopic investigation over the past few years<sup>5,6</sup>. The current



study aimed to give a complete outline of the optimized molecule structure, the vibrational assignments, electronic characteristics like an energy gap, a HOMO, a LUMO and an electrostatic molecular potential of the titled compound. In order to calculate the number of vibrational waves, the optimized molecular structure was used in B3LYP method. This paper focuses on the spectral characterization of the title molecules<sup>7-8</sup>. The correlation between the title molecular structure, bioactivity and Non-Linear optical characters are also decoded with quantum chemical calculations. A systematic approach presents unique applications of quantum mechanical method in the analysis of sum biological important piperidine derivatives compounds.

### Computational details

The compound was optimized with 6-31G (d, p) basis set using DFT/B3LYP quantum chemical methods. For the calculation of frontier molecular orbitals, a time-dependent DFT (TD-DFT) method was used<sup>9-11</sup>. DFT (B3LYP/6-311++G (d, p) method has been employed in this work to calculate optimized molecular structure, vibrational descriptions and charge transfer of the titled molecule. DFT calculations were significantly employed in electronic molecular structure treatment. The investigation was done under 6311++G is the basis (d, p) because of an efficient and cost effective level<sup>12</sup>. The complete computation has been carried out on personal computers involved with the Gaussian 09W programme package.

## RESULTS AND DISCUSSION

### Molecular geometry

Gaussian 09 and Gauss view programme provides all the optimized structure and numbering of atoms in the selected molecule. The bond length and bond angles of the optimized molecule are calculated with the basis set of HF/B3LYP using 6-31G. The calculated B3LYP values are higher than HF levels. The bond length and angles are presented in Table 1. Considering the energy-optimized geometry of the molecular derived from both basis set, the conceptual values of this method for correlation were taken up and are dependable. The C-C and C-H bond distances of piperidine ring were in the range of 1.555–1.516 Å and 1.112–1.094 Å respectively, whereas, the optimized C-C-C and C-C-H bond angles were in the range of 113.60–109.99° and

111.12–103.57° respectively. The C-N and N-H bond distances were calculated in the range 1.09–1.07 Å and 1.01 Å, 0.9 Å, also calculated the (126.6°) C–C–C, (108.5°) N–C–C bond angles for the piperidine molecule. With regard to the Endo cyclic torsional angles, the optimized C–H lengths in the CH<sub>2</sub> groups are calculated using the B3LYP method in the 1.092 Å range. In addition, calculation outcome shows that the geometric parameter calculated is in good understanding with the remaining geometric parameters.

**Table 1: Optimized some geometrical parameters of 2,6 dithenobenzene-3-enyl 3,5 dimethyl piperidine-4-one bond length (Å), bond angles (°) and dihedral angle**

Atom Bonds	Value	
	HF/6-31G	B3LYP/6-31G
Optimized Parameters (Angstroms and degrees)		
Bond Lengths		
C1-C2	1.5417	1.549
C1-C3	1.5251	1.5497
C1-C26	1.5373	1.5495
C1-H28	1.0828	1.0962
C2-N4	1.4588	1.476
C2-C7	1.5524	1.5645
C2-H29	1.0924	1.1072
C3-C5	1.5251	1.5296
C3-O27	1.1952	1.2445
N4-C6	1.4588	1.476
N4-H30	0.997	1.0156
C5-C6	1.5416	1.5495
C5-C25	1.5373	1.5496
C5-H31	1.0828	1.0962
C6-C16	1.5525	1.5645
C6-H32	1.0924	1.1072
C7-C8	1.5208	1.5243
C7-C9	1.5452	1.5491
C7-H33	1.0862	1.0988
C8-C10	1.3913	1.4065
C8-C12	1.3849	1.4001
C9-S11	1.826	1.9153
C9-H34	1.0826	1.092
C9-H35	1.0814	1.091
C10-S11	1.7736	1.8414
C10-C14	1.3826	1.3937
C12-C13	1.3876	1.4022
C12-H36	1.0756	1.0854
C13-C15	1.3851	1.3998
C13-H37	1.0752	1.0848
C14-C15	1.3868	1.4023
C14-H38	1.0751	1.0844
C15-H39	1.0756	1.0852
C16-C17	1.5452	1.5491
C16-C18	1.5207	1.5243
C16-H40	1.0862	1.0988
C17-S19	1.826	1.9154

Continue Tabel 1

C17-H41	1.0814	1.091	<b>Continue Tabel 1</b>		
C17-H42	1.0826	1.092	C7-C9-H34	110.5167	111.741
C18-C20	1.3913	1.4065	C7-C9-H35	113.9293	114.0752
C18-C21	1.3849	1.4001	S11-C9-H34	108.4989	107.264
S19-C20	1.7736	1.8414	S11-C9-H35	108.4278	107.2119
C20-C23	1.3826	1.3937	H34-C9-H35	108.4586	109.6694
C21-C22	1.3876	1.4023	C8-C10-S11	112.7779	112.8978
C21-H43	1.0756	1.0854	C8-C10-C14	121.492	121.8204
C22-C24	1.3851	1.3997	S11-C10-C14	125.7023	125.2487
C22-H44	1.0752	1.0848	C9-S11-C10	90.0302	88.3309
C23-C24	1.3867	1.4024	C8-C12-C13	120.0829	120.1154
C23-H45	1.075	1.0844	C8-C12-H36	120.3126	120.1069
C24-H46	1.076	1.0852	C13-C12-H36	119.6043	119.777
C25-H47	1.0833	1.094	C12-C13-C15	120.1718	120.2002
C25-H48	1.0823	1.0936	C12-C13-H37	119.7916	119.7407
C25-H49	1.0862	1.0966	C15-C13-H37	120.0358	120.0579
C26-H50	1.0833	1.094	C10-C14-C15	118.8108	118.6902
C26-H51	1.0862	1.0966	C10-C14-H38	120.6631	120.7737
C26-H52	1.0823	1.0936	C15-C14-H38	120.5133	120.5219
<b>Bond Angles</b>			C13-C15-C14	120.419	120.3971
C2-C1-C3	112.6602	112.9138	C13-C15-H39	119.9713	120.0557
C2-C1-C2	113.4293	112.9987	C14-C15-H39	119.5938	119.533
C2-C1-H28	109.5428	109.2076	C6-C16-C17	111.0768	110.8205
C3-C1-C26	108.8228	109.1232	C6-C16-C18	115.6384	114.8327
C3-C1-H28	103.5984	104.3159	C6-C16-H40	106.6519	106.0655
C26-C1-C28	108.2511	107.8063	C17-C16-C18	103.8824	105.4939
C1-C2-N4	107.6346	107.8015	C17-C16-H40	109.4246	109.3534
C1-C2-C7	114.4285	114.2842	S11-C6-H40	110.1082	110.25
C1-C2-H29	108.5329	108.5148	C16-C17-S19	106.8607	106.504
N4-C2-C7	107.8985	108.0588	C16-C17-H41	113.9237	114.0758
N4-C2-H29	110.6928	110.8025	C16-C17-H42	110.5226	111.7475
C7-C2-H29	107.6648	107.3984	S19-C17-H41	108.4244	107.2059
C1-C3-C5	121.4356	121.7206	S19-C17-H42	108.5014	107.2615
C1-C3-O27	119.2528	119.0697	H41-C17-H42	108.4605	109.6715
C5-C3-O27	119.2543	119.0698	C16-C18-C20	114.1291	114.8709
C2-N4-C6	113.3893	114.0966	C16-C18-C21	126.912	126.4244
C2-N4-H30	110.7439	113.1252	C20-C18-C21	118.9463	118.7039
C6-N4-H30	110.7426	113.1234	C17-S19-C20	90.0328	88.3325
C3-C5-C6	112.6526	112.9207	C18-C20-S19	112.7783	112.90
C3-C5-C25	108.8214	109.1214	C18-C20-C23	121.4924	121.82
C3-C5-H31	103.6013	104.3184	S19-C20-C23	125.7017	125.24
C6-C5-C25	113.4331	112.9869	C18-C21-C22	120.0826	120.116
C6-C5-H31	109.5412	109.2149	C18-C21-H43	120.3129	120.109
C25-C5-H31	108.2554	107.804	C22-C21-H43	119.6042	119.773
N4-C6-C5	107.6327	107.8064	C21-C22-C24	120.172	120.200
N4-C6-C16	107.8921	108.0583	C21-C22-H44	119.792	119.738
N4-C6-H32	110.6928	110.8017	C24-C22-H44	120.035	120.059
C5-C6-C16	114.4384	114.2844	C20-C23-H24	118.810	118.690
C5-C6-H32	108.5313	108.5122	C20-C23-H45	120.662	120.773
C16-C6-H32	107.6647	107.3971	C24-C23-H45	120.510	120.520
C2-C7-C8	115.6256	114.8313	C22-C24-C23	120.419	120.39
C2-C7-C9	111.0861	110.8269	C22-C24-H46	119.9703	120.05
C2-C7-H33	106.6554	106.0653	C23-C24-C6	119.5948	119.533
C8-C7-C9	103.8774	105.4896	C5-C25-H47	110.0854	110.034
C8-C7-H33	110.1134	110.2515	C5-C25-H48	110.9354	110.593
C9-C7-H33	109.4246	109.3515	C5-C25-H49	111.232	111.107
C7-C8-C10	114.1275	114.8713	H47-C25-H48	108.4952	108.594
C7-C8-C12	126.9138	126.4214	H47-C25-H49	108.3015	108.491
C10-C8-C12	118.9461	118.7066	H48-C25-H49	107.6915	107.939
C7-C9-S11	106.8619	106.5058	C1-C26-H50	110.0866	110.030
<b>Continue Tabel 1</b>			C1-C26-H51	111.2336	111.107

C1-C26-H52	110.9326	110.596	<b>Continue Tabel 1</b>		
H50-C26-H51	108.3029	108.492	C25-C5-C6-C16	96.88	97.44
H50-C26-H52	108.4945	108.593	C25-C5-C6-H32	-23.36	-22.35
H51-C26-H52	107.6908	107.941	H31-C5-C6-N4	95.71	97.61
Dihedral Angles			H31-C5-C6-C16	-24.18	-22.52
C3-C1-C2-N4	18.959	18.03	H31-C5-C6-H32	-144.44	-142.32
C3-C1-C2-C7	138.86	138.16	C3-C5-C25-H47	55.31	54.87
C3-C1-C2-H29	-100.88	-102.02	C3-C5-C25-H48	175.41	174.84
C26-C1-C2-N4	143.15	142.48	C3-C5-C25-H49	-64.73	-65.30
C26-C1-C2-C7	-96.94	-97.37	C6-C5-C25-H47	-178.44	-178.6
C26-C1-C2-H29	23.30	22.42	C6-C5-C25-H48	-58.34	-58.65
H28-C1-C2-N4	-95.78	-97.53	C6-C5-C25-H49	61.50	61.19
H28-C1-C2-C7	24.12	22.60	H31-C5-C25-H47	56.65	-57.84
C8-C1-C2-H29	144.37	142.40	H31-C5-C25-H48	63.44	62.12
C2-C1-C3-C5	25.33	26.01	H31-C5-C25-H49	-176.70	-178.02
C2-C1-C3-O27	-157.43	-158.32	N4-C6-C16-C17	75.44	73.03
C26-C1-C3-C5	-101.35	-100.53	N4-C6-C16-C18	-166.50	-167.56
C26-C1-C3-O27	75.86	75.12	N4-C6-C16-H40	-43.71	-45.55
H28-C1-C3-C5	143.62	144.46	C5-C6-C16-C17	-164.79	-166.9
H28-C1-C3-O27	-39.14	-39.87	C5-C6-C16-C18	-46.75	-47.56
C2-C1-C26-H50	178.45	178.69	C5-C6-C16-H4	76.04	74.44
C2-C1-C2-H51	-61.49	-61.14	H32-C6-C16-C17	-44.06	-46.54
C2-C1-C26-H52	58.35	58.71	H32-C6-C16-C18	73.98	72.85
C3-C1-C26-H50	-55.29	-54.81	H32-C6-C16-H40	-163.22	-165.1
C3-C1-C26-H51	64.75	65.35	C2-C7-C8-C10	96.21	95.56
C3-C1-C6-H52	-175.39	-174.78	C2-C7-C8-C12	-85.09	-84.76
H28-C1-C26-H50	56.66	57.90	C9-C7-C8-C10	-25.75	-26.76
H28-C1-C26-H51	176.72	178.07	C9-C7-C8-C12	152.92	152.9
H28-C1-C26-H52	-63.43	-62.06	H33-C7-C8-C10	-142.84	-144.7
C1-C2-N4-C6	-69.72	-68.05	H33-C7-C8-C12	35.84	34.95
C1-C2-N4-H30	165.07	160.73	C2-C7-C9-S11	-89.28	-89.45
C7-C2-N4-C6	166.30	167.95	C2-C7-C9-H34	152.84	153.7
C7-C2-N4-H30	41.10	36.74	C2-C7-9C-H35	30.44	28.60
H29-C2-N4-C6	48.73	50.54	C8-C7-C9-S11	35.65	35.40
H29-C2-N4-H30	-76.46	-80.66	C8-C7-C9-H34	-82.21	-81.42
C1-C2-C7-C8	46.79	47.58	C8-C7-C9-H35	155.38	153.4
C1-C2-C7-C9	164.83	166.98	H33-C7-C9-S11	153.21	153.9
C1-C2-C7-H33	-75.99	-74.42	H33-C7-C9-H34	35.34	37.13
N4-C2-C7-C8	166.55	167.58	H33-C7-C9-H35	-87.05	-87.97
N4-C2-C7-C9	-75.40	-73.02	C7-C8-C10-S11	3.713	4.68
N4-C2-C7-H33	43.76	45.56	C7-C8-C10-C14	-178.09	-177.3
H29-C2-C7-C8	-73.93	-72.83	C12-C8-C10-S11	-175.08	-175.0
H29-C2-C7-C9	44.10	46.55	C12-C8-C10-C14	3.10	2.99
H29-C2-C7-H33	163.26	165.14	C7-C8-C12-C13	178.57	177.7
C1-C3-C5-C6	-25.30	-26.04	C7-C8-C12-H36	-1.51	-2.50
C1-C3-C5-C25	101.39	100.48	C10-C8-C12-C13	-2.71	-2.53
C1-C3-C5-H31	-143.58	-144.52	C10-C8-C12-H36	177.18	177.1
O27-C3-C5-C6	157.47	158.29	C7-C9-S11-C10	-30.26	-28.8
O27-C3-C5-C25	-75.83	-75.171	H34-C9-S11-C10	88.91	90.8
O27-C3-C5-H31	39.18	39.81	H35-C9-S11-C10	-153.47	-151.3
C2-N4-C6-C5	69.76	68.01	C8-C10-S11-C9	15.98	14.5
C2-N4-C6-C16	-166.26	-167.99	C14-C10-S11-C9	-162.11	-163.3
C2-N4-C6-H32	-48.69	-50.58	C8-C10-C14-C15	-1.21	-1.25
H30-N4-C6-C5	-165.03	-160.77	C8-C10-C14-H38	-179.92	-179.8
H30-N4-C6-C16	-41.05	-36.78	S11-C10-C14-C15	176.72	176.5
H30-N4-C6-H32	76.50	80.6	S11-C10-C14-H38	-1.98	-2.1
C3-C5-C6-N4	-19.02	-17.96	C8-C12-C13-C15	0.50	0.42
C3-C5-C6-C16	-138.92	-138			
C3-C5-C6-H32	100.80	102.00			
C25-C5-C6-N4	-143.21	-142.4			
<b>Continue Tabel 1</b>					

C8-C12-C13-H37	-179.83	-179
H36-C12-C13-C15	-179.32	-179
H36-C12-C13-H37	0.33	0.32
C12-C13-C15-C14	1.41	1.35
C12-C13-C15-H39	179.9	179
H37-C13-C15-C14	-178.23	-178
H37-C13-C15-H39	0.30	0.3
C10-C14-C15-C13	-1.05	-0.93
C10-C14-C15-H39	-179.60	-179.5
H38-C14-C15-C13	177.64	177.70
H38-C14-C15-H39	-0.90	-0.93
C6-C16-C17-S19	89.31	89.4
C6-C16-C17-H41	-30.40	-28.58
C6-C16-C17-H42	-152.81	-153.7
C18-C16-C17-S19	-35.64	-35.40
C18-C16-C17-H41	-155.36	-153.45
C18-C16-C17-H42	82.23	81.43
H40-C16-C17-S19	-153.20	-153.95
H40-C16-C17-H41	87.08	87.98
H40-C16-C17-H42	-35.32	-37.12
C6-C16-C18-C20	-96.22	-95.55
C6-C16-C18-C21	85.08	84.76
C17-C16-C18-C20	25.74	26.76
C17-C16-C18-C21	-152.93	-152.91
H40-C16-C18-C20	142.83	144.72
H40-C16-C18-C21	-35.85	-34.95
C16-C17-S19-C20	30.25	28.88
H41-C17-S19-C20	153.45	151.37
H42-C17-S19-C20	-88.93	-90.90
C16-C18-C20-S19	-3.70	-4.69
C16-C18-C20-C23	178.09	177.29
C21-C18-C20-S19	175.09	175.01
C21-C18-C20-C23	-3.10	-2.99
C16-C18-C21-C22	-178.65	-177.79
C16-C18-C21-H43	1.51	2.51
C20-C18-C21-C22	2.71	2.54
C20-C18-C21-H43	-177.11	-177.15
C17-S19-C20-C18	-15.98	-14.53
C17-S19-C20-C23	162.11	163.39
C18-C20-C23-C24	1.21	1.25
C18-C20-C23-H45	179.92	179.89
S19-C20-C23-C24	-176.72	-176.49
S19-C20-C23-H45	1.97	2.13
C18-C21-C22-C24	-0.50	-0.42
C18-C21-C22-H44	179.84	179.97
H43-C21-C22-C24	179.32	179.27
H43-C21-C22-H44	-0.32	-0.33
C2-C22-C24-C23	-1.41	-1.35
C2-C22-C24-H46	-179.95	-179.98
H44-C22-C24-C23	178.23	178.24
H44-C22-C24-H46	-0.30	-0.37
C20-C23-C24-C22	1.05	0.94
C20-C23-C24-H46	179.60	179.57
H45-C23-C24-C22	-177.64	-177.69
H45-C23-C24-H46	0.90	0.93

### Vibrational Assignments

A total of 52 atoms and 150 vibrational frequencies are observed in the spectroscopic study. The spectroscopic vibrational modes are calculated by HF and DFT/6-311+G (d, p) basis set. The frequencies, intensities of IR, Raman and characteristic group frequencies have also been calculated. In organic chemistry, vibrational spectroscopy is used to detect functional group<sup>13</sup>. It is also used to study molecular tests, kinematics, etc. The molecules, however are made up of different vibration modes, there is therefore a various vibrational spectrum in the study of the title molecule. Fig. 2 and 3 show the calculated frequencies. Table 2 shows the calculated and observed vibrational assignments with the HF and the B3LYP/6-311++G method.

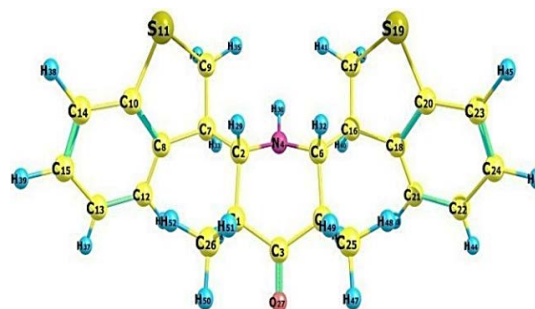


Fig. 1. Optimized structure of the organic molecule obtained at B3LYP/6-31G level of theory

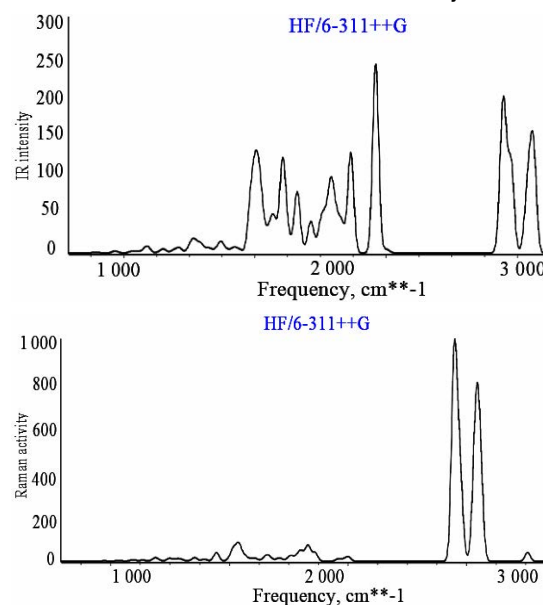


Fig. 2. Theoretical vibrational spectrum using HF/6-311+G for title molecule

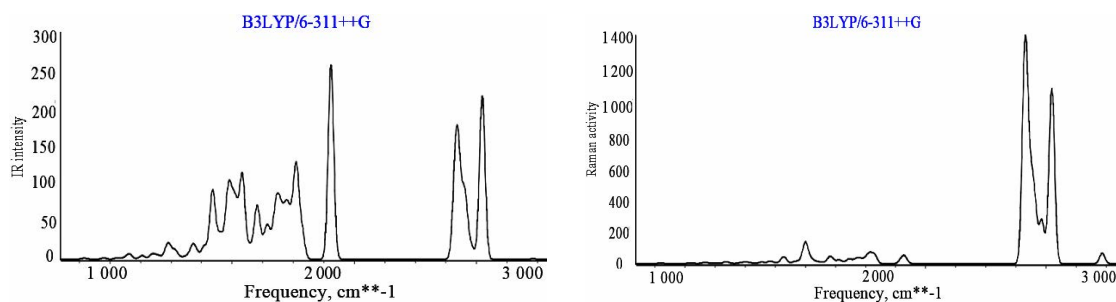


Fig. 3. Theoretical vibrational spectrum using B3LYP/6-311++G for title molecule

Table 2: Calculated vibrational frequencies ( $\text{cm}^{-1}$ ) and assignments title compound based on HF/6-311++G (d, p) and B3LYP/6311++G (d, p) methods

HF		B3LYP		Vibrational Assignments
6-311G	6-311++G	6-311G	6-311++G	
-229.9653	-229.9015	-234.9466	-219.1928	Ring deformation
-197.7089	-197.4371	-208.4349	-190.6649	C-C wagging and ring Deformation
-64.792	-66.0186	-124.1784	-51.1752	Ring stretching
-41.0665	-41.8883	-106.4637	17.6728	Ring bending
58.4204	60.062	-99.7258	54.9081	C=O wagging and ring Twisting
75.373	75.0479	42.3406	63.7788	C=O wagging and ring Twisting
99.3333	101.0364	66.7223	94.9203	C=O wagging and ring Twisting
154.7052	153.7594	116.391	134.5907	Ring breathing and twisting
178.8022	177.8274	141.2279	158.0064	Ring bending
183.9821	183.2629	146.8225	159.746	Ring stretching and C-H rocking
189.8117	188.5251	158.6888	165.8716	Ring stretching
208.9179	209.0036	187.1049	190.4608	Ring stretching
237.4691	237.5488	199.3726	205.6494	Ring deformation and C-H rocking
266.7524	266.3947	228.7993	233.6933	Ring stretching
272.5417	272.3757	238.9764	245.5082	Ring breathing
288.6973	288.0281	248.7996	257.3432	C-S out plan bending
306.8084	306.0891	269.2158	267.4396	Ring deformation and C-H rocking
350.3618	350.9602	323.1495	319.4722	Ring deformation
376.0731	377.3177	339.3296	335.6433	C-H rocking
389.7852	389.8144	343.792	341.0143	Ring stretching
395.046	395.5424	360.9819	356.6177	C-H rocking and ring Deformation
422.4164	423.1322	363.2598	360.3997	C-H rocking and ring Deformation
429.9013	428.2786	390.2312	387.322	Ring deformation
484.0331	482.8366	418.927	406.004	C-H rocking
493.7563	494.1814	459.9176	451.7972	Ring deformation
514.0624	513.339	463.8629	458.6466	Ring deformation and C-H rocking
519.1581	518.1794	466.8887	464.5253	Ring deformation
538.5809	537.9589	490.1502	483.1624	Ring deformation
550.413	549.7329	502.5644	494.4182	Ring deformation
567.5258	567.3939	510.3295	501.7365	Ring deformation and C-H wagging

Continue Tabel 2

582.7368	583.9799	531.9834	530.0417	Ring stretching
600.9812	600.1037	539.9461	535.6637	Ring breathing
616.14	616.7398	561.7379	553.4781	Ring deformation
627.203	627.1937	575.4665	568.9549	Ring deformation
646.0239	645.6668	589.3565	581.1875	Ring deformation
655.1498	654.5796	603.8106	594.485	Ring deformation and N-H rocking
698.1099	697.7662	642.6309	632.4736	Ring deformation and C-H rocking
702.0815	701.5741	647.9494	635.5417	Ring deformation and C-H rocking
714.0517	713.8855	649.8632	637.1369	Ring deformation and C-H rocking
740.462	740.6503	687.0236	672.6354	Ring deformation and C-H rocking
744.1232	744.0099	689.0506	677.9077	Ring deformation and C=O,N-H wagging
785.8559	786.7782	727.7485	706.1245	Ring deformation and C-H rocking
791.3242	791.3688	731.4054	713.5378	Ring deformation and C-S stretching
839.1609	840.0747	753.0798	765.2063	C=O, N-H wagging and ring deformation
870.9846	869.9239	791.343	774.9497	Ring deformation and C-H wagging
881.1406	881.3927	792.3548	776.3088	Ring deformation and C-H rocking
892.4164	892.1166	829.1346	816.7441	Ring breathing and C-H rocking
914.724	914.705	841.0573	825.0769	Ring breathing and C-H rocking
968.5293	966.2263	862.8071	839.9625	C-H wagging
996.142	994.4025	875.8364	847.6034	C-H wagging
1000.018	999.8391	891.3911	893.2602	Ring breathing and C-H bending
1005.7455	1005.3395	908.6649	902.956	Ring deformation and C-H wagging
1021.3447	1021.7178	949.602	925.617	C-H twisting and C-S stretching
1032.097	1033.9909	964.1402	935.1974	C-S stretching
1034.5141	1036.325	977.5419	950.2878	C-H wagging
1044.7215	1045.3036	987.4671	958.3716	C-H wagging
1057.2137	1057.681	989.5713	968.7278	C-H twisting
1078.7418	1079.0423	998.8103	982.6365	Ring deformation and C-H rocking
1086.7718	1087.4327	1003.6359	986.2575	Ring breathing and C-H twisting
1095.0551	1095.8576	1013.132	1000.3396	Ring breathing
1104.1023	1103.1149	1033.6935	1011.2327	Ring deformation and C-H twisting
1116.1952	1115.5555	1040.6599	1015.7436	Ring deformation and C-H rocking
1123.0419	1123.4044	1046.1253	1017.5342	Ring deformation and C-H rocking
1128.275	1129.2571	1052.0511	1022.2435	Ring deformation and C-H rocking
1132.8151	1133.3653	1053.9672	1027.8967	Ring deformation and C-H rocking
1136.4018	1137.4183	1061.0005	1031.9701	Ring deformation and C-H rocking

Continue Tabel 2

1138.8026	1138.944	1061.7903	1038.7215	Ring deformation and C-H rocking
1149.4985	1149.7295	1076.3219	1052.9522	Ring deformation and C-H rocking
1174.7591	1174.0216	1079.659	1058.2829	Ring deformation and C-H twisting
1177.4643	1177.3652	1087.926	1065.6865	Ring deformation and C-H rocking
1186.2782	1186.3641	1100.8396	1083.9865	Ring deformation and C-H twisting
1192.9383	1193.1815	1103.1899	1085.0626	Ring deformation and C-H rocking
1193.7124	1194.7236	1130.4886	1109.2998	Ring deformation and C-H wagging and rocking
1212.3907	1210.1853	1143.4984	1122.4819	Ring deformation and C-H rocking
1213.6868	1211.2829	1150.3136	1128.6193	Ring deformation and C-H twisting
1226.1481	1224.5593	1165.8715	1139.0741	Ring deformation and C-H rocking
1235.7552	1234.6732	1172.9482	1142.1047	C-H bending
1260.5388	1258.0619	1178.5707	1149.614	Ring deformation and C-H rocking
1279.8835	1277.546	1185.4593	1167.0785	Ring deformation and C-H wagging
1305.1793	1304.1336	1195.6647	1181.6884	Ring deformation and C-H twisting
1310.901	1309.6981	1223.7745	1198.9568	Ring deformation and C-H rocking
1323.6257	1320.8807	1230.3274	1205.3265	Ring deformation and C-H rocking
1334.0922	1331.7754	1238.3741	1205.8497	Ring deformation and C-H rocking
1338.3194	1335.5194	1251.4193	1227.2436	Ring deformation and C-H rocking
1342.9036	1340.1095	1255.4694	1228.631	C-H twisting and wagging
1348.5897	1346.8178	1266.4931	1238.9583	C-H twisting and rocking
1381.9072	1378.3352	1272.0954	1242.1408	C-H twisting and rocking
1400.2423	1395.7662	1281.4487	1245.7012	C-H twisting and rocking
1415.1201	1412.235	1285.594	1262.0967	C-H twisting
1420.8765	1417.899	1300.6325	1268.0356	C-H wagging
1425.1358	1421.0844	1307.8837	1277.7265	C-H wagging
1431.8808	1429.0995	1310.5914	1290.8372	C-H twisting
1436.6867	1434.0305	1325.1579	1296.0829	C-H twisting
1447.8105	1445.6143	1336.6448	1308.1699	C-H rocking
1494.91	1492.5972	1368.7083	1337.9642	C-H wagging
1512.7839	1509.2183	1378.6874	1351.1258	C-H wagging
1517.5159	1514.8413	1389.4823	1357.1497	C-H wagging
1523.0336	1519.6343	1394.0807	1366.8168	C-H twisting
1531.587	1528.0701	1403.0751	1369.4993	C-H Wagging
1549.5016	1541.9211	1411.9181	1379.2735	C-H Wagging
1567.0541	1560.6581	1430.6842	1390.1801	C-H Wagging
1567.5519	1562.0163	1433.5468	1393.8097	C-H Wagging
1570.3472	1567.9337	1435.7215	1409.3893	C-H rocking
1581.7624	1577.566	1446.5708	1417.6663	C-H Wagging
1586.0539	1582.3054	1456.4304	1427.632	C-H Wagging
1587.7337	1584.0311	1459.948	1438.6632	C-H rocking
1595.4597	1592.1041	1473.682	1444.8595	C-H rocking
1603.1257	1599.8848	1475.1923	1446.3295	C-H Wagging
1610.5187	1607.148	1482.1595	1449.7688	C-H rocking

Continue Tabel 2

1613.0798	1608.8684	1484.7331	1451.7971	C-H Wagging
1613.8459	1609.7811	1496.3276	1467.7979	C-H Wagging
1626.5013	1621.3002	1499.5117	1471.5591	C-H rocking
1642.0802	1637.7192	1511.4255	1482.1718	C-H rocking
1655.5896	1651.8691	1531.0755	1497.2362	C-H bending
1657.8567	1655.6736	1532.3556	1501.4131	C-H bending
1661.2425	1658.9591	1535.5841	1504.857	C-H bending
1664.4556	1660.9151	1547.6845	1523.0464	N-H bending
1668.8901	1665.5444	1552.7418	1524.1664	C-H bending
1678.7874	1675.2564	1557.3609	1535.1664	C-H rocking
1722.0965	1720.0198	1563.1688	1537.6116	Ring deformation and C-H
1727.1414	1725.064	1592.3086	1571.1272	Bending Ring vibration
1734.8125	1731.6091	1597.9645	1575.8544	C-H bending Ring vibration
1928.6092	1920.2172	1810.5681	1792.4077	C-H bending
C-H Wagging				
1975.8466	1974.1168	1839.9844	1809.6942	Ring deformation
2007.1174	2005.5411	1858.1994	1828.6638	C-H Wagging
C-H Wagging				
2868.4597	2870.0092	2795.3312	2816.6257	C-H symmetric Stretching
2879.9917	2879.9549	2801.5365	2822.418	C-H Symmetric Stretching
2881.5956	2883.5014	2804.7972	2831.4775	C-H Asymmetric Stretching
2891.1491	2892.8767	2810.7297	2835.1639	C-H Symmetric Stretching
2893.1229	2893.476	2823.5487	2848.9838	C-H Symmetric Stretching
2895.05	2896.9	2826.5636	2851.9813	C-H Symmetric Stretching
2912.5909	2914.9605	2852.112	2875.7023	C-H Asymmetric Stretching
2913.9058	2916.2647	2853.5064	2876.6501	C-H Symmetric Stretching
2919.5906	2921.949	2858.3856	2881.0983	C-H Asymmetric Stretching
2921.0254	2923.5672	2859.0394	2882.1881	C-H Asymmetric Stretching
2934.2185	2934.3405	2865.9662	2884.1242	C-H Asymmetric Stretching
2946.8574	2948.1615	2883.7547	2902.3975	C-H symmetric Stretching
2947.8394	2949.3087	2885.4393	2904.5105	C-H Asymmetric Stretching
2953.0494	2954.3067	2886.3938	2905.7117	C-H Stretching
2958.2998	2959.8465	2903.499	2920.3287	C-H Asymmetric Stretching
3059.1811	3059.7431	2947.2746	2962.7994	C-H Asymmetric Stretching
3069.196	3065.3724	3005.9766	3027.1185	C-H Asymmetric Stretching
3069.4009	3065.6188	3006.2641	3027.4497	C-H Asymmetric Stretching
3082.6205	3079.2146	3017.6493	3036.9308	C-H Asymmetric Stretching
3082.864	3079.4807	3017.9073	3037.2391	C-H Asymmetric Stretching
3100.1909	3096.564	3031.4313	3047.9356	C-H Asymmetric Stretching
3100.3236	3096.7068	3032.8139	3049.4982	C-H Asymmetric Stretching
3125.0966	3123.3264	3035.8762	3050.0402	C-H Stretching
3127.4855	3125.7954	3037.5426	3052.6164	C-H Stretching
3509.2952	3514.3522	3448.0997	3464.4121	N-H Stretching

### C–H vibrations

A C–H stretching vibration in the region 3,100–3000  $\text{cm}^{-1}$ <sup>14</sup> has been shown by the hetero aromatic structure. This is the only area where the C-H stretching vibration can be identified. The nature of the substitutions in this region does not greatly affect the bands. Due to the influence from N-H stretching vibration, which was found very dominant in this molecule. The vibrational frequency in the region of 2816-1142  $\text{cm}^{-1}$  was evident of title molecule in this study. In the expected range of vibration, the functional group vibrations were observed.

### N-H vibration

The N-H stretching frequencies of vibration

are always higher than the other stretching vibrations, and the length of the bond is smaller than the length of other molecules. Usually N-H stretching vibrations<sup>15</sup> are continued at 3500-3300  $\text{cm}^{-1}$  for any heterocyclic compound. Six vibrational modes are required by nitrogen hydrogen bonds and this is part of the entire vibrational pattern. The N-H vibration takes place in the area 3464  $\text{cm}^{-1}$  in this research. This is due to strong hydrogen bonding during the gas phase, whereas in the solid phase it is absent.

### C=O vibrations

The C=O stretching vibration band visualized from the carboxylic group in which the C=O stretching position is dependent on physical

state, mass and electronic effects, intermolecular and intra molecular hydrogen bonding<sup>16</sup>, usually in this region between 1750 and 1700  $\text{cm}^{-1}$ . This band position determines the bond strength of the hydrogen. In this research the carboxyl group, assigned below 1000  $\text{cm}^{-1}$  in the region, are directly linked to its electronic structure as well as its geometric positioning. The effect of the inductive, mesomeric and conjugating efficiency in both inter and intermolecular factors on carbonyl absorption of frequent organic compounds.

### C-C Vibrations

The visible spectrum of the benzene and its derivatives, the ring vibration is very remarkable and characteristic of the aromatic ring itself. This is not so much because of the nature of the substituent but because of the way the chain is substituted. In this study, the title molecule found that the region is generally observed below 700  $\text{cm}^{-1}$  at external vibration bending. The chains vibrations were observed at 190  $\text{cm}^{-1}$ .

### Ring vibrations

The benzene ring has six stretching vibration. The bending vibration of the benzene ring in the plane and out of the plane is usually seen in the literature below 1000  $\text{cm}^{-1}$ , and those modes are non-pure but are significantly affected by other vibrations. The title molecule affects to a great extent the in-plan and out-of-plane bending modes of the rings, producing bands less than 600  $\text{cm}^{-1}$ .

### C-S vibrations

The C-S stretching bands are normally noticed in the range of 670–930  $\text{cm}^{-1}$ . For our study, the title compound shows the frequency range from 713 to 935  $\text{cm}^{-1}$ . The out-of-plane C-S bending vibrations bands are predicted in the regions 420–320  $\text{cm}^{-1}$ , respectively. In the current research work, the C-S out of plane bending vibrations are assigned to below 300  $\text{cm}^{-1}$ . All the C-S vibrational bands of the molecule are well determined with the previous research work. Also, the observed values by B3LYP/6-311++G (d, p) are almost related to the computed values.

### Mulliken atomic charge

The effect of atomic charges determines the molecular polarization, dipole moment, electronic structure and few molecular system properties.

The classification of charges across the atoms proposes that donor and recipient pair molecules are established. The investigation of Mulliken atomic charges plays a vital role in the implementation of quantum chemicals in the molecular system. Fig. 4 shows the Mulliken charge arrangement structure of the title compound. The negative charge carrier is more in oxygen and Sulphur atoms, while positive charge occupies all hydrogen atoms. In addition, the S19 atom has a greater electron-negative (-0.38886e) charge than the S11 atom in Mulliken atomic chargers. This is because the electron-negative Sulphur atom is present. Thus Mulliken population analysis interprets the reaction behavioral analysis of various chemicals.

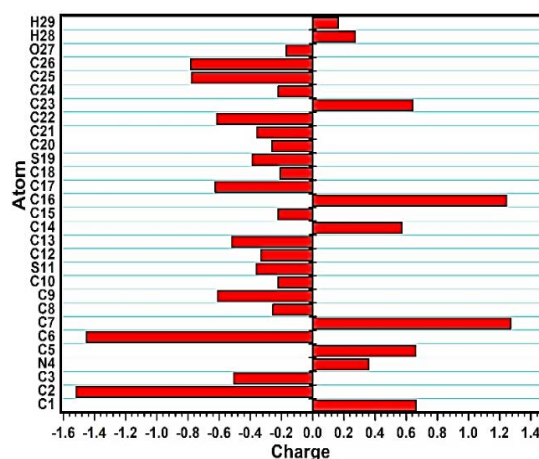


Fig. 4. Schematic representation of Mulliken atomic charges

### Frontier molecular orbitals

The frontier molecular orbitals play an important role in understanding the electrical and optical properties of the titled molecule. The HOMO energy defines the ability to supply electrons while the LUMO shows that electrons can be accepted. The molecular chemical ability is defined by the HOMO-LUMO gap. A molecule with a small energy gap in the orbit is more polarized and usually combined with the high chemical responsiveness. The energy gap between HOMO and LUMO is more influential for structural stability. Fig. 5 shows the difference in energy level between HOMO and LUMO. The estimated energy difference is 9.3387eV. This wide energy gap therefore means high excitement, good stability and high chemical durability.

HOMO energy = -8.4165eV

LUMO energy = 0.9222eV HOMO-LUMO energy gap = 9.3387eV

The smaller energy band gap increases the chemical activity of the titled molecule. The HOMO-LUMO energy and its gap are determined using HF/6-11++G (d, p) level.

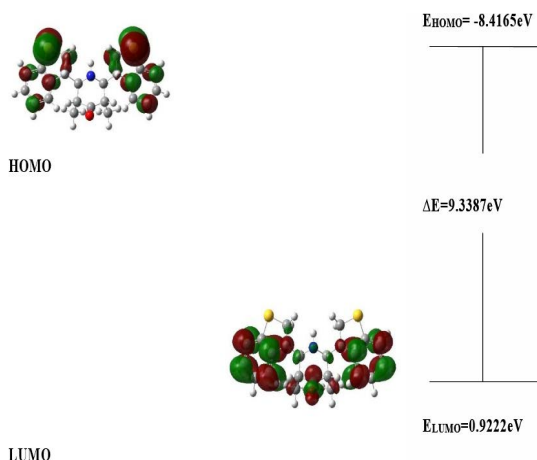


Fig. 5. The frontier molecular orbitals of title molecule

### Molecular orbital studies

Furthermore, the difference of energy band values is known to help us identify the chemical reactivity and stability of titled molecule. The energy band gap of the molecule is small and this gap is usually combined with a high reactivity of chemicals and a low kinetic stability. In terms of the degree of orbital reactivity of the atom<sup>17</sup> the quantum chemical calculations are performed. Mulliken was introduced a new formulation, which allowed to extend the concept to molecules, in terms of two further periodic properties, namely ionizing potentials and affinity. The affinity of electron refers exactly to the ability to accept an electron. The greater

HOMO-LUMO gap means a hard molecule, and a smaller HOMO-LUMO gap means a soft molecule, due to its chemical hardness. The reactivity of the selected compound is also associated with the molecule's hardness. The values of ionization and electron affinity are calculated with both HOMO and LUMO. For Mulliken electron negativity, the mean of HOMO and LUMO energy value can be used. The index of electrophility is the amount of energy reduction due to the greater electron movement between donor and recipient. The values of electronegativity, chemical potential, chemical hardness, softness, and electrophility index are 3.74715 eV, -3.74715 eV, 4.66935eV, 0.107081eV, 1.503543eV, respectively, for the title Compound.

### Thermodynamic Parameters

Several thermodynamic parameters such as heat capacity, entropy and enthalpy changes for the titled compound were determined using, the DFT/B3LYP with 6-31G (d, p) basic sets. Such estimated frequencies of the title compound provide the information of all structural thermodynamic characteristics including rotational constants, null point vibration power, heat capacity, and entropy<sup>18</sup>. These values are calculated using the basis set of 6-311++G (d, p) levels using B3LYP and HF method and presented in the Table 3. For further understanding the selected molecules, the collected thermodynamic parameters are used to analysis the thermodynamic functional relationships and the direction of chemical reactions in accordance with the thermodynamics law.

Table 3: The calculated thermodynamic parameter of title molecule

Basis set	HF 6-311G	HF 6-311++G	B3LYP 6-311G	B3LYP 6-311++G
Zero-Point Vibrational	290.6913	290.4561	273.5251	271.3272
Energy(Kcal mol-1)	0.34304	0.34304	0.34304	0.34304
Rotational Constants	0.09194	0.09194	0.09194	0.09194
Frequency (GHz)	0.07810	0.07810	0.07810	0.07810
Specific heat(Cv) (Cal mol-1K-1)	72.466	72.518	78.239	83.756
Entropy(S) (Cal mol-1K-1)	128.996	128.979	133.915	143.786
Dipole Moment $\mu$ (Debye)	4.7568	4.6720	4.0293	3.6527

### Molecular electrostatic potential (MEP) mapping

The electrostatic potential diagram illustrates the probability that the electron densities are integrated throughout the system. In other words, it provides functional information to the reactive section. Electrophilic and nucleophilic molecular system centers are suitable for the development of

biochemical system. The electrostatic potential of the title compound shown in Fig. 6. The molecular surface contours are also illustrated in Fig. 7. The region with the most negative potential is shown in a red colour in the MEP diagram, while the blue colour shows the most positive potential surface. Red, blue, light blue, yellow and green are shown on the surface of the MEP.

Red surface is electron-rich and moderately negative; blue, electron-deficient and partially positive; light-blue, light electron-deficient; yellow colour; a type of region rich in electrons; and green, neutral.

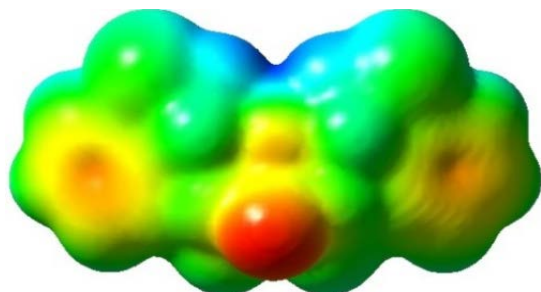


Fig. 6. Molecular electrostatic potential surface

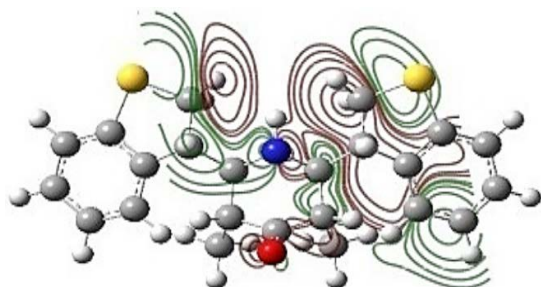


Fig. 7. MEP contour of titled molecule

### Hyperpolarizability studies

As an extensive tool for research on spectroscopy analysis, hyper polarizability and the non-linear optical properties of the titled molecule of potential NLO materials are considered. Non-linear response, Hyperpolarizability ( $\beta_{ijk}$ ) and linear polarization ( $\alpha_{ij}$ ) of first order may be furnished as Taylor expansion in the form  $\mu_{tot} = \mu_0 + \alpha_j E_j + \beta_{ijk} E_j E_k + \dots$

The dipole moment ( $\mu$ ), mean polarizability ( $\alpha$ ) and the first order Hyperpolarizability ( $\beta$ )<sup>19</sup> for the titled molecule is illustrated using following equations:

$$\mu = \sqrt{(\mu_x^2 + \mu_y^2 + \mu_z^2)}$$

$$\alpha = \frac{(\alpha_{xx} + \alpha_{yy} + \alpha_{zz})}{3}$$

$$\beta = [(\beta_{xxx} + \beta_{xyy} + \beta_{xzz})^2 + (\beta_{yyy} + \beta_{yzz} + \beta_{yxx})^2 + (\beta_{zzz} + \beta_{zxx} + \beta_{zyy})^2]^{(1/2)}$$

The estimated dipole moment, mean polarizability and first order hyperpolarization of first-order values are 7,478 Debye, 0,402 Å esu and  $1,4024 \times 10^{-31} \text{ cm}^5 \text{ esu}^{-1}$ . A  $\beta$ -electron donor-to-

acceptor movement which makes the molecule highly polarizable as a vital behavior for NLO activities<sup>20</sup>.

### CONCLUSION

The results presented and discussed in the report of procedure seemed appropriate to be summarized. The theoretical analysis of DFT provides information on the orbital interactions and vibrational frequency systems, nature of the electronic structure, functional groups. In the organic synthesis of perfume, drugs, dyes and pharmaceuticals, heterocyclic compounds play significant role. The use of such a base set of 6-311 and 6-311++ is available to optimize the geometry of piperidine products by HF and DFT/B3LYP methods. The computed data is based on proof of the gaseous phase. The different calculated bonding angles are satisfactorily compatible with the normal values. The B3LYP/6-311++G (d, p), then used to generate dependable geometry and associated piperidine derivatives properties. The method further tends to produce a vibration analysis. The orbital bond analysis provides the natural structure of Lewis with maximum accuracy. The highest rate of electron density will be achieved. In addition, the HOMO-LUMO band gap assists the molecule's biologically active properties. It provides information on the distribution of the charge density and differentiates the chemical molecule reactivity. The mapping electron density with electrostatic potential surface has been achieved to explain the size, the shape, the charging density distribution and the location of the chemical reactivity of the molecules. Finally, the Hyperpolarizability of the tile compound is analyzed for optical industrial applications.

### ACKNOWLEDGMENT

We are extremely indebted to Dr. Sudha Mohan ram, Principal of Sri Eshwar College of Engineering, Coimbatore for the steadfast encouragement during all stages of our research to realize our work into reality.

### Conflict of Interest

The authors claim no conflict of interest in the current research work.

## REFERENCES

1. Subbagh H.I. El, AbuZaid S.M., Mahran M.A., Badira F.A, Alobaid A.M., *J. Med. Chem.*, **2000**, *43*, 2915–2921.
2. Jeron B.R., Spencer K.H., *Eur. Pat. Appl. Ep.*, **1988**, *27*, 7794.
3. Perumal R.V., Adiraj M., Shanmugapandiyan P., *Indian Drugs.*, **2001**, *38*, 156-159.
4. Hagenbach R.E., Gysin H., *Experiential.*, **1952**, *8*, 184-185.
5. Katritzky A.R., Fan W. J, *J. Org. Chem.*, **1990**, *55*, 3205-3209.
6. Ganelin C.R., Spickett R.G, *J. Med. Chem.*, **1965**, *8*, 619-625.
7. Savithiri.S, Arockia doss.M, Rajarajan. G, Thanikachalam.V, Bharanidharan.S, Saleem. H, *Spectrochim. Acta Part A.*, **2015**, *136*, 782-792.
8. Arockia doss.M, Savithiri.S, Rajarajan.G, Thanikachalam.V, Saleem.H, *Spectrochim. Acta Part A.*, **2015**, *148*, 189-202.
9. Arockia doss.M, Savithiri.S, Rajarajan.G, Thanikachalam.V, Saleem.H, *Spectrochim. Acta Part A.*, **2015**, *151*, 773-784.
10. Anandhy.K, Arockia doss.M, Savithiri.S, Rajarajan.G, Mahalakshmi.S, *Int. J. Adv. Res. Trends Eng. Technol.*, **2016**, *3*(2), 1301-1311.
11. Stratmann.R. E, Scuseria G.E, Frisch. M. J, *J. Chem. Phys.*, **1998**, *109*, 8218-8224.
12. Miertus. S, Tomasi. J, *J. Chem. Phys.*, **1982**, *65*, 239-245.
13. Snehalatha.M, Ravi Kumar. Joe C, I.H., Sekar.N, Jayakumar V.S, *Spectrochim. Acta Part A.*, **2009**, *72*, 654-662.
14. Varsanyi.G, *Vibrational Spectra of Benzene Derivatives*, Academic Press, Newyork., **1980**.
15. Chandra. S, Saleem. H, Sudaraganesan. N, Sebastian. S, *Spectrochim Acta.*, **2008**, *A74* 704-713.
16. Mohanbabu. B, Bharathikannan. R, Siva. G, *J Mater Sci: Mater Electron.*, **2017**, *28*, 13740–13749.
17. Nabil Elleuch, Walid Amamou, Ali Ben Ahmed, Younes Abid, Habib Feki, *J. Spect. Chem. Acta Part A.*, **2014**, *128*, 781.
18. Govindarajan M., Karabacak M., Udayakumar V., Periandy S., *“Spectrochimica Acta Part A.*, **2012**, *88*, 37.
19. Zhang R, Dub B, Sun G, Sun Y, *Spectrochim. Acta A.*, **2010**, *75*, 1115.
20. Ramalingam S, Periandy S, Mohan S, *Spectrochimica Acta Part.*, **2010**, *A 77*, 73.